IEEE Access
Multidisciplinary | Rapid Review | Open Access Journal

Received March 24, 2021, accepted March 31, 2021, date of publication April 8, 2021, date of current version June 29, 2021.

Digital Object Identifier 10.1109/ACCESS.2021.3071916

A 2-D Hybrid FE Model With Double Air Gap Elements for Eccentric Magnetic Harmonic Gears

JUNDA ZHANG AND YUEJIN ZHANG
Shanghai University, Shanghai 201900, China
Corresponding author: Yuejin Zhang (zhangyj@shu.edu.cn)

ABSTRACT Eccentric magnetic harmonic gears with high gear ratios exhibit high torque densities. However, the revolution and rotation of the eccentric rotor increase the magnetic field analysis complexity. This paper presents a hybrid finite element approach of magnetic field analysis for magnetic harmonic gears. The eccentric air gap region has been divided into three parts: two uniform layers, adjoining the stator and the rotor respectively, are treated as air gap elements; one non-uniform middle layer, as a variable air gap permeance, is discretized by FE meshes similar to the stator and the rotor. Mesh reconstruction can be avoided because the annular cylindrical rings of the two air gap elements are introduced. The mixed eccentric motion of the rotor can be easily treated. In order to save the computational time an equivalent motion mode is introduced and the sliding surface technique is applied by which the coefficient calculation of the air gap elements only needs to be done once wherever the rotor moves. The torques are calculated from the flux densities of the air gap elements. A prototype test confirms the validity of the prediction, and the accuracy of the obtained results is evaluated with FEM.

INDEX TERMS Hybrid finite element method, double air-gap element, eccentric magnetic harmonic gear.

I. INTRODUCTION

Magnetic gears have many great potential advantages over mechanical gears, including lubricant-free, low noise, reduced maintenance, and inherent overload protection. Based on the flux modulation principle magnetic harmonic gears can achieve high torque densities and high efficiency with high gear ratios [1]. Active torque densities of up to 150 kNm/m^3 have been demonstrated for eccentric magnetic harmonic gears (EMHG) with high gear ratios [2], [3]. Torque densities of as much as 291 kNm/m^3 can be achieved with a flux-focusing rotor topology [4].

A high accurate computation of the magnetic fields and torques in magnetic harmonic gears is the subject of great importance. However, the biggest issue in the computation is how to facilitate the eccentric motion. The advantages of analytical methods, such as clear physical concepts, fast calculation, and no restriction from the meshes make magnetic field analysis easy, especially when the eccentric rotation of the rotor leads to non-uniform air gap [5]–[11]. A model with analytical method only can hardly handle nonlinear problems such as the saturation of ferromagnetic materials, though.

The associate editor coordinating the review of this manuscript and approving it for publication was Guido Lombardi.

The finite element method (FEM) can provide high precision results and be readily used with knowledge of the machine's geometry and material properties. But a pure numerical computation has to be repeated entirely for every relevant rotor position as the rotor moves in an orbital revolution around the stator's stationary central axis.

There are several methods to facilitate the movement of the rotor in FE analyses. The moving-band was first proposed in [12], and applicable for eccentric rotors [13], [14], but a new discretization in the band has to be constructed for each time step and thus the numbering as well as the amount of nodes in the mesh does not stay constant. The sliding surface technique is another practical approach to deal with the rotor movement [15]. However, this technique is only suitable for the interface between static and moved objects must be fixed. The air gap element (AGE) [16]–[19] is a technique whereby the field in the entire air gap region is calculated analytically using a Fourier series expansion of the vector potential. The advantages of the AGE technique over other methods are that the movement of the rotor is simplified and the accuracy of the torque calculation is believed to be superior to that of conventional FEM due to the high order of the field representation in the air gap region. The eccentric AGE approach and the sliding surface technique

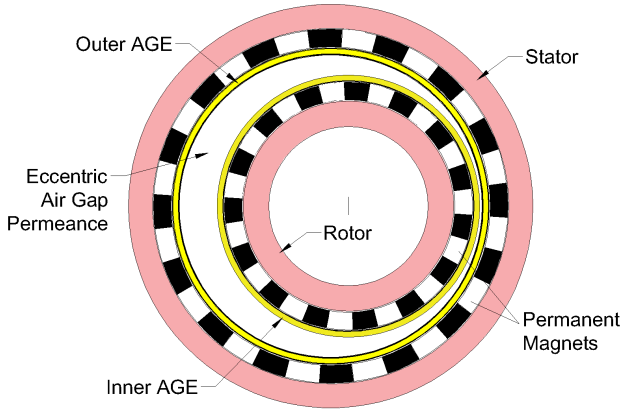

FIGURE 1. Construction of the magnetic harmonic gear.

are utilized with modeling of the magnetic bearings [20], and the formulation is solved by the iterative solution algorithm. However, the perturbation analysis appears reasonable only for small eccentricities. Since the higher-order terms in the series expression are eliminated, the eccentric AGE is an approximate model and not suitable to the EMHG with a large eccentricity.

A hybrid finite element with double AGEs approach is proposed in this paper. The eccentric air gap is subdivided into three parts. Two uniform air gap cylindrical annuluses, adjoining the stator and the rotor respectively, are treated as the AGEs. The non-uniform middle air gap layer is discretized by FE meshes similar to the stator and the rotor. Thus the eccentric movement of the rotor can be handled very easily. With the help of the application of the sliding surface technique the coefficient calculation of the AGE only needs to be done once wherever the rotor moves. Therefore the computational time is reduced. According to the Maxwell stress tensor theory the torque is calculated by the analytical expression. The test of a prototype with two stages confirms the validity of the method.

II. HYBRID MODELS

A EMHG is split into five domains(Fig. 1), where the eccentric air gap is divided into three regions. The two uniform annuluses are treated as air gap elements. The middle non-uniform air gap area, as a variable air gap permeance, is treated as FE region. Thus, the permanent magnet rotor along with the air gap permeance can be moved easily. A few assumptions are made in modeling process. 1) The static magnetic field and torque are analyzed, and the eddy current effects are neglected. 2) The PMs have linear demagnetization characteristics with relative permeability $\mu_r = 1.10$.

A. FINITE ELEMENT MODEL

The finite element discretization of the static Maxwell equations in the stator, the rotor and the air gap permeance domains, by triangular FE elements yields,

$$\boldsymbol{KA} = \boldsymbol{f} \tag{1}$$

where the homogenous Dirichlet conditions are considered in the stator and the rotor boundary surfaces. In(1), $\boldsymbol{K}$ is the FE stiffness matrix, $\boldsymbol{A}$ is the unknown vector associated with the magnetic vector potentials in the stator, the rotor and the air gap permeance domains, and $\boldsymbol{f}$ is a vector associated with permanent magnets.

B. AIR GAP ELEMENT MODEL

In the air gap cylindrical annulus, owing to the absence of excitation or magnetic material, the magnetic vector potentials satisfy the Laplace equation. The analytical solution with Dirichlet condition on the interfaces, in the case of a 2-D polar coordinate system, takes the form

$$A(r,\theta) = \sum_{i=1}^{N_s} \alpha_i(r,\theta) A_{si} - \sum_{j=1}^{N_r} \beta_j(r,\theta) A_{rj} \tag{2}$$

where N_s, N_r correspond to the number of nodes, and A_{si}, A_{rj} the nodal values of $\boldsymbol{A}$ on the outer and the inner interfaces, respectively. It is called the air gap element model since the potential in the air gap are expressed as the sum of the shape function times the nodal potential [16]–[18]. The shape functions of the AGE at i and j node, expressed as Fourier series, are

$$\begin{aligned}
\alpha_i(r,\theta) &= \frac{\ln(r/R_r)}{2\ln(R_s/R_r)} g_{a0i} \\
&\quad + \sum_{n=1}^{\infty} \frac{E_n(r,R_r)}{E_n(R_s,R_r)} \left(g_{ani}\cos n\theta + g_{bni}\sin n\theta\right) \\
\beta_j(r,\theta) &= \frac{\ln(r/R_s)}{2\ln(R_s/R_r)} h_{c0j} \\
&\quad + \sum_{n=1}^{\infty} \frac{E_n(r,R_s)}{E_n(R_s,R_r)} \left(h_{cnj}\cos n\theta + h_{dn}\sin n\theta\right)
\end{aligned} \tag{3}$$

where R_s, R_r are the radius of the outer and inner boundaries of the AGE respectively, and $E_n(u,v) = (u/v)^n - (v/u)^n$.

In(3), the Fourier coefficients (g, h) are computed by using linear interpolation of the vector potentials at the interface between two successive nodes, for example, at the external circle interface [19],

$$\begin{aligned}
g_{a0i} &= \frac{1}{\pi}(\eta_i + \eta_{i+1}) \\
g_{ani} &= -\frac{1}{\pi n^2}\left(\frac{\sin n\xi_i \sin n\eta_i}{\eta_i} - \frac{\sin n\xi_{i+1}\sin n\eta_{i+1}}{\eta_{i+1}}\right) \\
&\qquad i = 1, 2, \ldots N_s \\
g_{bni} &= \frac{1}{\pi n^2}\left(\frac{\cos n\xi_i \sin n\eta_i}{\eta_i} - \frac{\cos n\xi_{i+1}\sin n\eta_{i+1}}{\eta_{i+1}}\right)
\end{aligned} \tag{4}$$

where $\xi_i = (\theta_i + \theta_{i+1})/2$, $\eta_i = (\theta_{i+1} - \theta_i)/2$ and θ_i is the spatial angle of node i. The Fourier coefficient h of the inner circle interface are similar to those presented in (4). The magnetic field energy of one AGE is

$$W_a = \frac{1}{2}\nu_0 \int_\Omega B^2 d\omega = \frac{1}{2}\nu_0 \int_\Omega (\nabla \times A)^2 d\omega \tag{5}$$

where ν_0 is the air reluctivity, and Ω is the AGE region.

The function of the minimization equation of the air gap energy is determined from, for instance, the node i at the outer interface,

$$\frac{\partial W_a}{\partial A_{si}} = \frac{\pi \nu_0 L_{ef}}{2 \ln R_s/R_r}\left(\sum_k g_{a0k} g_{a0i} A_{sk} - \sum_j h_{c0j} g_{a0i} A_{rj}\right) + \pi \nu_0 L_{ef}\left\{\begin{array}{l}\sum_k \sum_n n \frac{P_n(R_s,R_r)}{E_n(R_s,R_r)}\left[g_{ank} g_{ant} + g_{bnk} g_{bni}\right] A_{sk} \\ -\sum_j \sum_n \frac{2n}{E_n(R_s,R_r)}\left[h_{cnj} g_{ani} + h_{dng} g_{bni}\right] A_{rj}\end{array}\right. \tag{6}$$

where L_{ef} is the axial length of the magnetic gear iron, and $P_n(u, v) = (u/v)^n + (v/u)^n$. The entire system equations to be solved can be completed when AGE and FE models are assembled by Dirichlet interface conditions.

C. ELECTROMAGNETIC TORQUE

The electromagnetic torque is given by Maxwell stress tensor as a function of radial and tangential components of the air gap magnetic density:

$$T_{em} = \frac{L_{ef}}{\mu_0}\int_0^{2\pi} r^2 B_r B_\theta d\theta \tag{7}$$

where r is the radius of an arbitrary circumference which lies in the air gap. The flux density is computed in the air gap by the derivative of the magnetic vector potentials, and then the electromagnetic torque can be derived from (2), (3)

$$T_{em} = \frac{2\pi L_{ef}}{\mu_0}\sum_{n=1}^{\infty}\frac{n^2}{E_n(R_s,R_r)} \times \left[\begin{array}{l}\left(\sum_{i=1}^{N_s} g_{bni} A_{si}\right)\left(\sum_{j=1}^{N_r} h_{cnj} A_{rj}\right) \\ -\left(\sum_{i=1}^{N_s} g_{ani} A_{si}\right)\left(\sum_{j=1}^{N_r} h_{dnj} A_{rj}\right)\end{array}\right] \tag{8}$$

This analytical expression shows that the value of the torque is independent of the radius r, and the order of this solution is of the same as the order of the solution of the vector potential, i.e. a profit in the accuracy of one order compared to the field quantities derived from the potential formulation using the first-order FE shape functions [21].

III. FREE ECCENTRIC MOTION OF THE ROTOR

With the introduction of the double AGEs there is no mesh restriction anymore among the stator, the rotor and the variable air gap permeance so that the rotor along with the variable air gap permeance can move freely. According to the movement principle of the EMHGs, when the high-speed rotor (the variable air gap permeance) rotates angle θ anticlockwise and the low-speed rotor rotates angle θ/p_r clockwise around its own central axis, where p_r is the pole pair of the low-speed rotor.

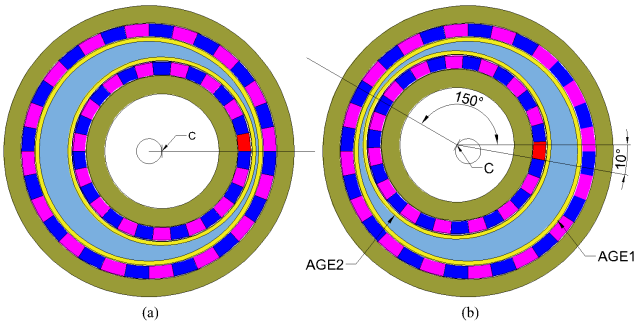

FIGURE 2. Relative positions between high-speed and low-speed rotors (a) 0°: 0° and (b) 150°: −10° ($p_r = 15$, c eccentric center).

It should be noticed that the center of the low-speed rotor, during the same period, will also rotate angle θ anticlockwise as shown in Fig. 2. Therefore the low-speed rotor makes a combined orbit and rotational motion, where the speed of the revolution is p_r times the speed of the rotation. The low-speed rotor moving, in the simulation, can be manipulated by two steps: the revolution first, that is the low-speed rotor and the variable air gap permeance rotate angle θ anticlockwise around the stator central axis; the second, only the permanent magnets of the low-speed rotor rotate angle $\theta + \theta/p_r$ around the rotor central axis clockwise while the variable air gap permeance keeps still. So the high-speed rotor and the low-speed rotor complete their own real movement respectively.

IV. COMPUTATIONAL EFFICIENCY IMPROVEMNET

A. COMPUTATIONAL TIME ANALYSIS

The FE model coupled with the AGE models results in a greatly increasing of the computational time. Two major factors affect the computational efficiency. One is a dense block appearing in the final system matrix which may have a drastic impact on the computational time, and the other is the recalculation of the air gap coefficients for every relevant rotor position as the rotor moves. Considering (4) and (6), the calculation of the air gap coefficients involves the circulation not only related to the number of nodes on AGE boundaries but also related to the number of Fourier series terms. The construction of the AGE sub-matrix needs next steps:

1 - $\xi_i = (\theta_i + \theta_{i+1})/2$, $\eta_i = (\theta_i - \theta_{i+1})/2$ for $i = 1$ to N_s

2 - g_{ani}, g_{bni} for $i = 1$ to N_s and for $n = 1$ to n_{max}

3 - Compute the coefficients of the AGE matrix by multiplying and summating calculation

4 - Construct a global matrix assembling AGE and FE contribution

The recalculation of the AGE matrix results in increasing computational time needed to solve the entire system equations obviously.

B. SLIDING SURFACE TECHNIQUE

The application of the sliding surface technique keeps the AGE coefficients unchanged when the rotor moves. In this

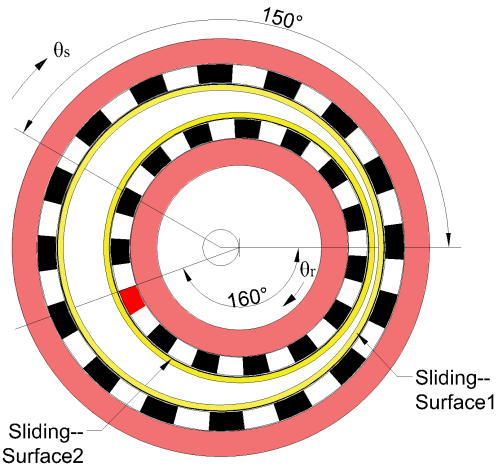

FIGURE 3. Equivalent motion in the reference frame of eccentric rotor central axis.

case, the AGE matrix needs to be calculated only once during the entire field computational process. Generally, the interface between the AGE and the moving object is selected as the sliding surface. The nodes on the AGE side are fixed while those on the moving object side are sliding. The magnetic vector potentials at the AGE and the moving object sides are related to each other by cyclic permutation rules. For convenience, an equidistant angular distribution of nodes is applied at the sliding surface.

C. EQUIVALENT MOTION MODE

Because of the eccentric orbital motion of the low-speed rotor, the sliding surface technique cannot be directly applied at the interfaces of the variant positions. An equivalent rotation mode is introduced in the paper by the alteration of the reference frame on the central axis of the low-speed rotor. From the new equivalent reference frame, the permanent magnets of the stator and the low-speed rotor will rotate around their own central axis in the same direction with different speeds (angles). When the stator rotates angle θ clockwise around the stator central axis, the low-speed rotor rotates angle $\theta + \theta/p_r$ clockwise around its own central axis at the same time(Fig. 3).

With the new reference frame the nodes on the AGE side are fixed and the AGE coefficients are invariable wherever the motion objects rotate. Therefore the double AGE matrices only need to be calculated once and are ready to be applied in all subsequent calculations.

V. SIMULATION AND TEST CONFIRMATION

A prototype dual-stage EMHG is built. The magnetic fields and electromagnetic torques of the prototype are computed by the proposed method. The parameters for the prototype are listed in Tab. 1.

Fig. 4 shows the flux line in the second stage calculated by the proposed method. The waveform of the radial flux densities calculated of the proposed method are in a good agreement with Ansys FEM, as shown in Fig. 5.

TABLE 1. Parameters of The Dual-stage Magnetic Harmonic Gear.

Parameter	First Stage	Second Stage
Stator inner diameter/mm	100	91
Rotor outer diameter/mm	76	67
Rotor inner diameter/mm	64	55
Stator and rotor PM thickness/mm	3.5	3.5
Rotor/Stator pole pairs	8/9	15/16
Average air-gap length/mm	5	5
Pole arc coefficient	1	1
PM remanence/T	1.25	1.25
Axial length/mm	20	20
Eccentric distance/mm	4	4

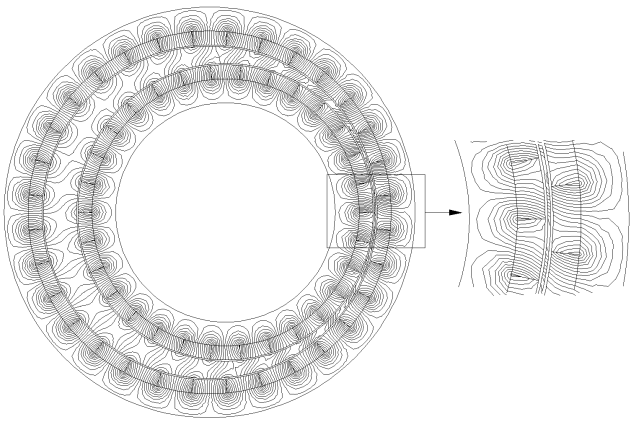

FIGURE 4. Flux line of the magnetic harmonic gear in the second stage.

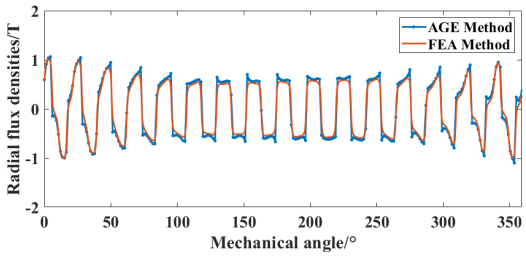

FIGURE 5. Waveforms of radial air-gap flux densities.

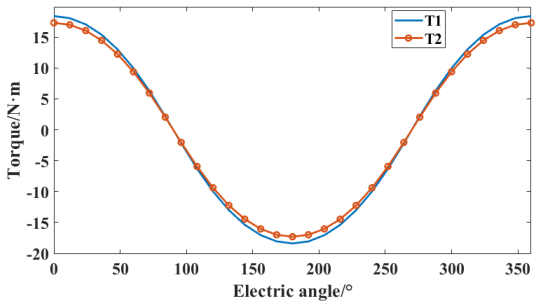

FIGURE 6. Torque-angle characteristic in the second stage.

Fig. 6 shows the torque-angle characteristic of the second stage. The static peak torques T1 and T2 calculated from the flux densities in the outer and inner AGEs are slightly different. The average of the gear ratio T1/T2 in the second stage is 1.0641, nearly equal to the pole-pairs ratio of the

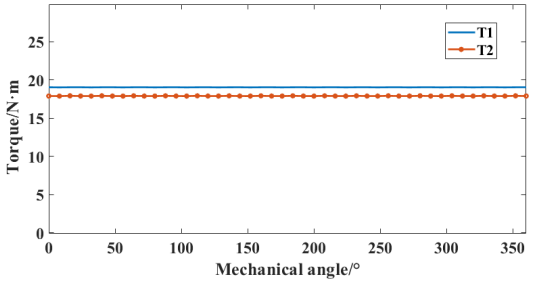

FIGURE 7. Variation of the peak-torque in the second stage.

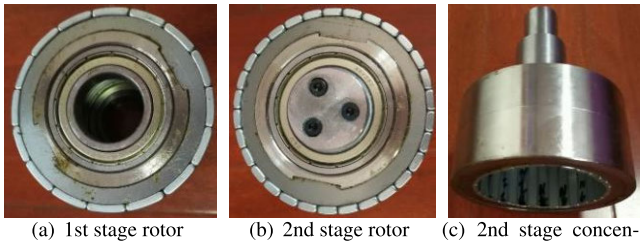

(a) 1st stage rotor (b) 2nd stage rotor (c) 2nd stage concentric outer rotor

FIGURE 8. Prototype components.

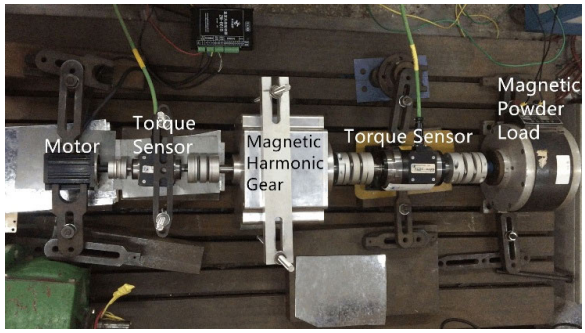

FIGURE 9. Test bench of the prototype.

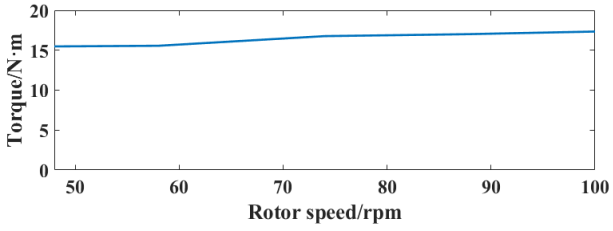

FIGURE 10. Measured torque-speed curve of the prototype.

stator and rotor [3], [22]. Fig. 7 shows the constant peak torque curves with the motion of the rotor.

The rotor components of the prototype and test bench are shown in Fig. 8 and 9. The output torque-speed measured curve in steady state is shown in Fig. 10. When the speed of the second stage rotor is 100rpm the output torque can reach 17.2N·m. The predicted peak torques and the computation time of 46 torque values by the proposed method and Ansys FEM are shown in Table 2.

The peak torques predicted by the proposed method and FEM are almost identical. The improved AGE method can

TABLE 2. Comparison of Hybrid AGE Method and FEM.

Method	Original AGE	Improved AGE	FEM
Peak Torque/N·m	18.90	18.90	18.87
Time/s	7870	2586	4278

save about 67% of computation time when compared with the original AGE method. And because much more time is spent on the mesh reconstruction every time rotor rotates, FEM is about 40% longer than the improved AGE method. It proves that the equivalent motion mode with the new reference frame makes the possibility of performing the application of the sliding surface technique and results in saving simulation time certainly.

Since the static torque-angle characteristic is nearly a sinusoidal curve (Fig. 6) the maximum output torque under the stable condition will be lower than the peak torque which occurs on the critical point of the torque-angle curve.

VI. CONCLUSION

The double AGEs model and the equivalent motion mode for EMHG are presented to consider the orbital revolution of the low-speed rotor and accelerate the field computation. In the first approach, the free eccentric motion of the rotor can be realized with no more new discretization in the air gap for every relevant rotor position. Second, the transition of the reference frame makes it possible to apply the sliding surface technique. Thereby, the AGE coefficients only need to be calculated once, which leads to an obvious decreasing overall computational time. The torque measurements of the prototype are presented to confirm the validity of the prediction of the proposed method.

REFERENCES

[1] F. T. Jorgensen, T. O. Andersen, and P. O. Rasmussen, "The cycloid permanent magnetic gear," *IEEE Trans. Ind. Appl.*, vol. 44, no. 6, pp. 1659–1665, Nov./Dec. 2008.

[2] J. Rens, R. Clark, S. Calverley, K. Atallah, and D. Howe, "Design, analysis and realization of a novel magnetic harmonic gear," in *Proc. 18th Int. Conf. Electr. Mach.*, Sep. 2008, pp. 1–4.

[3] J. Rens, K. Atallah, S. D. Calverley, and D. Howe, "A novel magnetic harmonic gear," *IEEE Trans. Ind. Appl.*, vol. 46, no. 1, pp. 206–212, Jan./Feb. 2010.

[4] K. Li, J. Bird, J. Kadel, and W. Williams, "A flux-focusing cycloidal magnetic gearbox," *IEEE Trans. Magn.*, vol. 51, no. 11, pp. 1–4, Nov. 2015.

[5] R. Liu, J. Tang, and Y. Zhang, "Air gap magnetic field calculation in eccentric magnetic harmonic gear," in *Proc. IEEE 2nd Int. Conf. Electron. Inf. Commun. Technol. (ICEICT)*, Jan. 2019, pp. 845–848.

[6] Y. Zhang, J. Zhang, and R. Liu, "Magnetic field analytical model for magnetic harmonic gears using the fractional linear transformation method," *Chin. J. Electr. Eng.*, vol. 5, no. 1, pp. 47–52, Mar. 2019.

[7] L. Jing, J. Gong, and T. Ben, "Analytical method for magnetic field of eccentric magnetic harmonic gear," *IEEE Access*, vol. 8, pp. 34236–34245, 2020.

[8] S. T. Boroujeni, S. P. Emami, and P. Jalali, "Analytical modeling of eccentric PM-inset machines with a slotless armature," *IEEE Trans. Energy Convers.*, vol. 34, no. 3, pp. 1466–1474, Sep. 2019.

[9] P. Jalali, S. T. Boroujeni, and N. Bianchi, "Simple and efficient model for slotless eccentric surface-mounted PM machines," *IET Electr. Power Appl.*, vol. 11, no. 4, pp. 631–639, Apr. 2017.

[10] F. Shakibapour, A. Rahideh, and M. Mardaneh, "2D analytical model for heteropolar active magnetic bearings considering eccentricity," *IET Electr. Power Appl.*, vol. 12, no. 5, pp. 614–626, May 2018.

[11] A. Hanic, D. Zarko, and Z. Hanic, "A novel method for no-load magnetic field analysis of saturated surface permanent-magnet machines using conformal mapping and magnetic equivalent circuits," *IEEE Trans. Energy Convers.*, vol. 31, no. 2, pp. 740–749, Jun. 2016.
[12] B. Davat, Z. Ren, and M. Lajoie-Mazenc, "The movement in field modeling," *IEEE Trans. Magn.*, vol. MAG-21, no. 6, pp. 2296–2298, Nov. 1985.
[13] A. Belahcen and A. Arkkio, "Computation of additional losses due to rotor eccentricity in electrical machines," *IET Electr. Power Appl.*, vol. 4, no. 4, pp. 259–266, 2010.
[14] C. Schlensok and G. Henneberger, "Calculation of force excitations in induction machines with centric and excentric positioned rotor using 2-D transient FEM," *IEEE Trans. Magn.*, vol. 40, no. 2, pp. 782–785, Mar. 2004.
[15] T. W. Preston, A. B. J. Reece, and P. S. Sangha, "Induction motor analysis by time-stepping techniques," *IEEE Trans. Magn.*, vol. 24, no. 1, pp. 471–474, Jan. 1988.
[16] A. Abdel-Razek, J. Coulomb, M. Feliachi, and J. Sabonnadiere, "The calculation of electromagnetic torque in saturated electric machines within combined numerical and analytical solutions of the field equations," *IEEE Trans. Magn.*, vol. MAG-17, no. 6, pp. 3250–3252, Nov. 1981.
[17] A. Abdel-Razek, J. Coulomb, M. Feliachi, and J. Sabonnadiere, "Conception of an air-gap element for the dynamic analysis of the electromagnetic field in electric machines," *IEEE Trans. Magn.*, vol. MAG-18, no. 2, pp. 655–659, Mar. 1982.
[18] T. J. Flack and A. Volschenk, "Computational aspects of time-stepping finite-element analysis using an air-gap element," in *Proc. Int. Conf. Elect. Mach.*, Paris, France, 1994, pp. 158–163.
[19] Y. Zhang, K. T. Chau, J. Z. Jiang, D. Zhang, and C. Liu, "A finite element–analytical method for electromagnetic field analysis of electric machines with free rotation," *IEEE Trans. Magn.*, vol. 42, no. 10, pp. 3392–3394, Oct. 2006.
[20] E. Schmidt, H. De Gersem, and T. Weiland, "Application of a computationally efficient air-gap element within the finite element analysis of magnetic bearings," *IEEE Trans. Magn.*, vol. 42, no. 4, pp. 1263–1266, Apr. 2006.
[21] K. Hameyer, R. Belmans, U. Pahner, and R. Mertens, "New technique to enhance the accuracy of 2-D/3-D field quantities and forces obtained by standard finite-element solutions," *IEE Proc.-Sci., Meas. Technol.*, vol. 145, no. 2, pp. 67–75, Mar. 1998.
[22] F. T. Jørgensen, "Design and construction of permanent magnetic gears," M.S. thesis, Fac. Eng. Sci., Philosophy Elect., Inst. Energy Technol., Aalborg Univ., Aalborg, Denmark, 2010.

JUNDA ZHANG was born in Shanghai, China, in 1986. He received the B.S. degree in automation engineering from Tongji University, Shanghai, in 2009, and the M.S. degree in control engineering from Shanghai University, Shanghai, in 2015, where he is currently pursuing the Ph.D. degree in electric machinery.

His research interests include magnetic field analysis, design of electrical machines, and permanent magnet brushless motor control.

YUEJIN ZHANG received the M.S. degree in electrical engineering from the Shanghai University of Technology, Shanghai, China, in 1988, and the Ph.D. degree in electrical engineering from Shanghai University, Shanghai, in 2005.

He is currently a Professor with Shanghai University, Shanghai. His research interests include magnetic field analysis, design of magnetic gears, and permanent magnet brushless and direct-drive electrical machines.